SCIENTIFIC REPORTS

OPEN

SUBJECT AREAS:
CANCER THERAPEUTIC RESISTANCE
CHEMOTHERAPY
MEMBRANE LIPIDS
BREAST CANCER

Received
12 March 2013

Accepted
20 May 2013

Published
6 June 2013

Correspondence and requests for materials should be addressed to G.A.K. (g.koning@erasmusmc.nl) or M.V. (m.verheij@nki.nl)

Defined lipid analogues induce transient channels to facilitate drug-membrane traversal and circumvent cancer therapy resistance

Albert J. van Hell[1], Manuel N. Melo[5], Wim J. van Blitterswijk[1], Dayana M. Gueth[1], Tanya M. Braumuller[3], Lilia R. C. Pedrosa[6], Ji-Ying Song[4], Siewert J. Marrink[5], Gerben A. Koning[6], Jos Jonkers[3] & Marcel Verheij[1,2]

[1]The Netherlands Cancer Institute – Antoni van Leeuwenhoek Hospital, Divisions of Biological Stress Responses, Plesmanlaan 121, 1066 CX Amsterdam, The Netherlands, [2]Radiotherapy, Plesmanlaan 121, 1066 CX Amsterdam, The Netherlands, [3]Molecular Pathology, Plesmanlaan 121, 1066 CX Amsterdam, The Netherlands, [4]Experimental Animal Pathology, Plesmanlaan 121, 1066 CX Amsterdam, The Netherlands, [5]Groningen Biomolecular Sciences and Biotechnology Institute and Zernike Institute for Advanced Materials, University of Groningen, Nijenborgh 7, 9747 AG Groningen, The Netherlands, [6]Laboratory Experimental Surgical Oncology, Section Surgical Oncology, Department of Surgery, Erasmus Medical Center, PO Box 2040, 3000 CA, Rotterdam, The Netherlands.

Design and efficacy of bioactive drugs is restricted by their (in)ability to traverse cellular membranes. Therapy resistance, a major cause of ineffective cancer treatment, is frequently due to suboptimal intracellular accumulation of the drug. We report a molecular mechanism that promotes trans-membrane movement of a stereotypical, widely used anti-cancer agent to counteract resistance. Well-defined lipid analogues adapt to the amphiphilic drug doxorubicin, when co-inserted into the cell membrane, and assemble a transient channel that rapidly facilitates the translocation of the drug onto the intracellular membrane leaflet. Molecular dynamic simulations unveiled the structure and dynamics of membrane channel assembly. We demonstrate that this principle successfully addresses multi-drug resistance of genetically engineered mouse breast cancer models. Our results illuminate the role of the plasma membrane in restricting the efficacy of established therapies and drug resistance - and provide a mechanism to overcome ineffectiveness of existing and candidate drugs.

The main barrier for a drug to diffuse over the body and enter its target cell is the plasma membrane. This barrier, enriched in sphingolipids and sterols, forms a dense hydrophobic sheet, almost impermeable for hydrophilic compounds[1,2]. In drug design, therefore, amphiphilicity is an essential molecular requirement (Lipinski's rules). Consequently, the number of potential drug candidates from the vast chemical space is greatly restricted[3,4], and the efficacy of existing drugs is limited[5,6]. Indeed, poor accumulation of cytotoxic drugs in tumour cells is a major limitation in cancer therapy, contributing to chemotherapy resistance.

Therefore, we questioned whether the membrane barrier function can be modulated in order to specifically enhance drug traversal and increase its therapeutic window. As this approach should be systemically applicable, we rationalized that the underlying mechanism requires concerted action with the drug molecule (instead of permeabilization for any compound). Doxorubicin is a stereotypical amphiphilic compound, whose membrane traversal is among the best characterized: the molecule's hydrophobic anthraquinone inserts into lipid bilayers spontaneously. Membrane translocation (flip-flop) of its hydrophilic daunosamine sugar, however, is slow and energetically unfavorable[7]. In the clinic, doxorubicin is widely used as an anti-cancer agent, but in various situations optimal efficacy is lacking. A long-circulating formulation, 100-nanometer pegylated liposomes (Doxil/Caelyx®), was developed to counteract the rapid plasma clearance of the free drug[8]. The liposomal entrapment significantly reduced toxicity (e.g. life-threatening cardiac failure), however failed to improve efficacy[9].

The short-chain sphingolipid analogues N-hexanoyl-sphingomyelin and N-octanoyl-glucosylceramide (GC) strongly enhance the intracellular accumulation of doxorubicin[10], which we found not to be due to trivial phenomena, such as non-specific detergent-like membrane fluidization[11]; however, any underlying mechanism remained obscure.

Here, we develop a paradigm of facilitated drug-membrane translocation based on defined lipid analogues; the mechanism is elucidated at molecular detail. Moreover, plasma membrane targeting, by systemic co-administration of GC, widens the therapeutic window of doxorubicin and overcomes multi-drug resistance.

Results

Membrane traversal of doxorubicin is facilitated by defined truncated phospho- and glycolipids. We previously demonstrated that GC acts at the level of the plasma membrane to enhance doxorubicin accumulation in the cell, but not by inhibition of ATP-dependent drug efflux pumps[11]. We first questioned whether GC acts entirely independent on membrane proteins. To that end, we developed a doxorubicin translocation assay using model membranes of well-defined lipid compositions in absence of proteins (Fig. S1A–D). In liquid-disordered palmitoyl oleoyl phosphatidylcholine (POPC)/cholesterol (CH) membranes, incorporation of GC significantly decreased doxorubicin translocation half-time ($p < 0.05$) (Fig. 1A). The effect of GC was even more pronounced in entirely liquid-ordered di-palmitoyl phosphatidylcholine (DPPC)/sphingomyelin (SM)/CH membranes, which by themselves are most impermeable for doxorubicin (Fig. 1A). In a POPC/CH/SM composition, where the liquid-disordered phase co-exists with liquid-ordered (rigid) domains, like in plasma membranes[1], the overall effect of GC was intermediate (Fig. S1E). These data show that lipid organization of the membrane, independent of proteins, determines the degree of GC-enhanced doxorubicin translocation.

We next determined the molecular requirements of the lipid analogues to facilitate membrane traversal of doxorubicin. Using BAEC cells, we first compared the effect of GC with that of other short-chain (phospho) lipids. While di-myristoyl-phosphatidylcholine (PC) only minimally affected the intracellular accumulation of doxorubicin over 1 hour, di-nonanoyl-PC substantially elevated this accumulation in a dose-dependent manner, similar to GC (Fig. 1B). We next varied in a series of sphingo- and glycerophospholipids the total aliphatic chain volume (i.e. the two acyl chains in PC, or acyl plus sphingosine hydrocarbon chain in sphingolipids) and the headgroup size, thus ranging from a strongly conical to an entirely cylindrical molecular geometry (see for definition of these geometries ref. 12). Fig. 1C shows that 25–27 carbons were optimal for

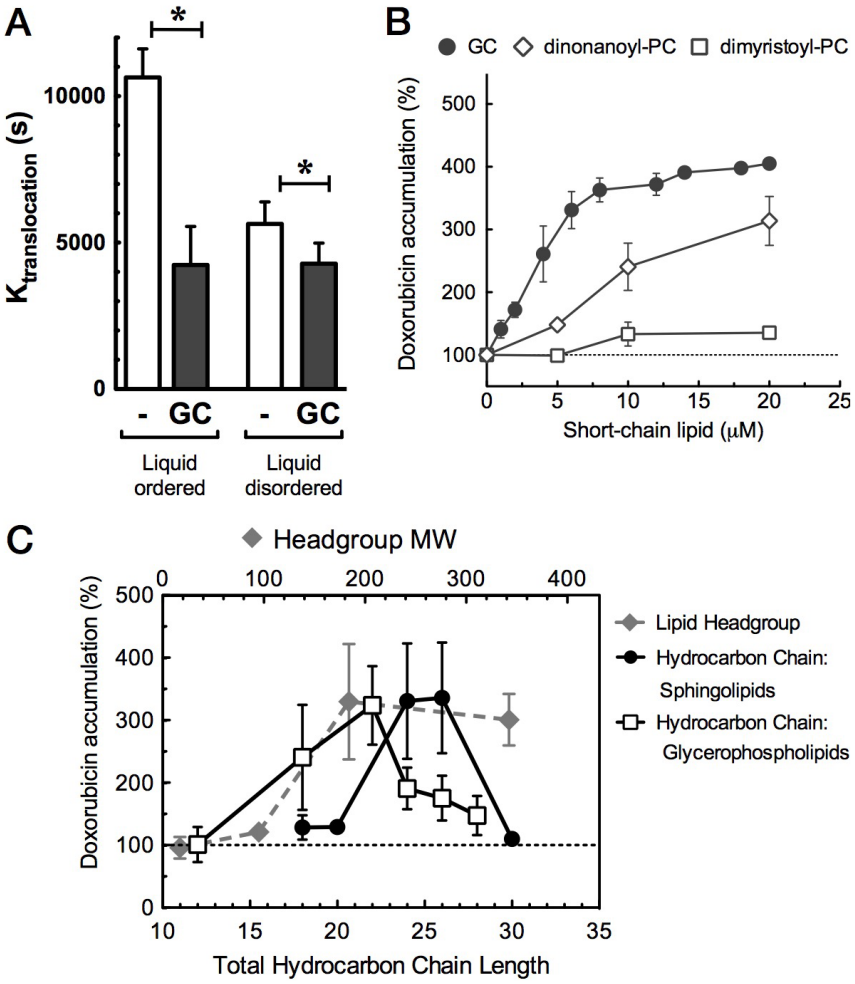

Figure 1 | Short-chain glycero- and sphingolipids facilitate doxorubicin-membrane traversal, depending on (A) membrane biophysical environment, (B, C) total acyl chain length, and (C) lipid headgroup size. (A). Doxorubicin translocation over liquid-ordered (DPPC: SM: Chol, 2 : 2 : 1 molar ratio) or liquid-disordered (POPC:Chol, 7 : 3 molar ratio) DNA-enclosed large unilamelar vesicles was determined in a fluorescence quenching assay (see Supplemental). GC significantly reduced translocation half-time (K(translocation) (in seconds; SEM, n = 3; $p < 0.05$). (B). Confluent BAEC cells were pre-incubated for 15 min with short-chain sphingolipid (GC) or phosphatidylcholines (PC 9 : 0/9 : 0 and PC 14 : 0/14 : 0), and doxorubicin was applied for 60 min. Intracellular doxorubicin accumulation was quantified (% of control, no lipid added) (SD, n = 5). (C). Doxorubicin accumulation in BAEC cells is plotted against the total hydrocarbon chain length (solid lines) at constant headgroup size (180 Da, phosphocholine or glucose); or against head group size at constant total chain length of 24–26 carbons (dashed line), using C6-Cer (17 Da; OH-group), C8-Cer-1-P (95 Da), C6-SM (184 Da), C8-LacCer (342 Da) (headgroup size in brackets); (mean, SD, n = 5).

sphingolipids, whereas around 22 carbons appeared most effective in case of glycerophospholipids. The shift of the optimum peak is well explained by the 3 carbons in the glycerol backbone of the glycerophospholipids.

With respect to the hydrophilic head group, at a constant total sphingolipid chain length of 24–26 C atoms, a minimum size of 180 Da was required for optimal doxorubicin accumulation (Fig. 1C, Table S1). Together, our findings indicate that analogues of natural lipids as defined by molecular geometry, are capable of enhancing doxorubicin traversal over preferentially the liquid-ordered lipid (raft) constituent of the plasma membrane.

Short-chain lipids assemble a transient membrane channel, facilitating doxorubicin traversal. The mechanism behind facilitated doxorubicin traversal by short-chain lipids, and the contribution of the drug molecule was investigated in silico using molecular dynamics (MD) simulations. This technique provides detailed insight in the behavior and interaction of individual molecules in lipid bilayers[13]. Lipid bilayers were modeled at atomic detail in the presence or absence of 20% short-chain di-octanoyl-phosphatidylcholine (PC 8 : 0/8 : 0; DOctPC). In line with experimental data[14], doxorubicin insertion and translocation over the membrane caused disordering of the local lipid and acyl chain organization (Fig. 2A, Movie S1). The presence of DOctPC caused a visible broadening and stabilization of such membrane perturbation, assembling a transient lipid channel for doxorubicin traversal. This DOctPC-mediated gateway afforded substantial solvation of doxorubicin (its daunosamine sugar in particular) within the lipid bilayer core, which involved lipid headgroups lining the pore's lumen and water molecules remaining associated with the sugar moiety (Fig. 2B, Movie S1).

Free energy landscapes were obtained for the translocation of doxorubicin across the lipid bilayers (Fig. 2C). Binding from the bulk phase (>3.0 nm distance to the center of the lipid bilayer) to the membrane surface (1.5–2.5 nm) is energy-favorable, by more than −25 kJ/mol, and indifferent for the presence of the short-chain lipids. Translocation of doxorubicin across the bilayer center (0.0 nm), on the other hand, surmounts an energy barrier of 45 kJ/mol for pure DPPC bilayers. This net energy barrier of 20 kJ/mol is in good agreement with reported data[7]. The presence of the short-chain lipids significantly reduced the net energetic barrier almost two-fold, by 7.8 kJ/mol (Fig. 2C).

We next determined the distribution of the DOctPC in the membrane in relation to the position of doxorubicin. When doxorubicin localized at the water-bilayer interface (membrane surface), no

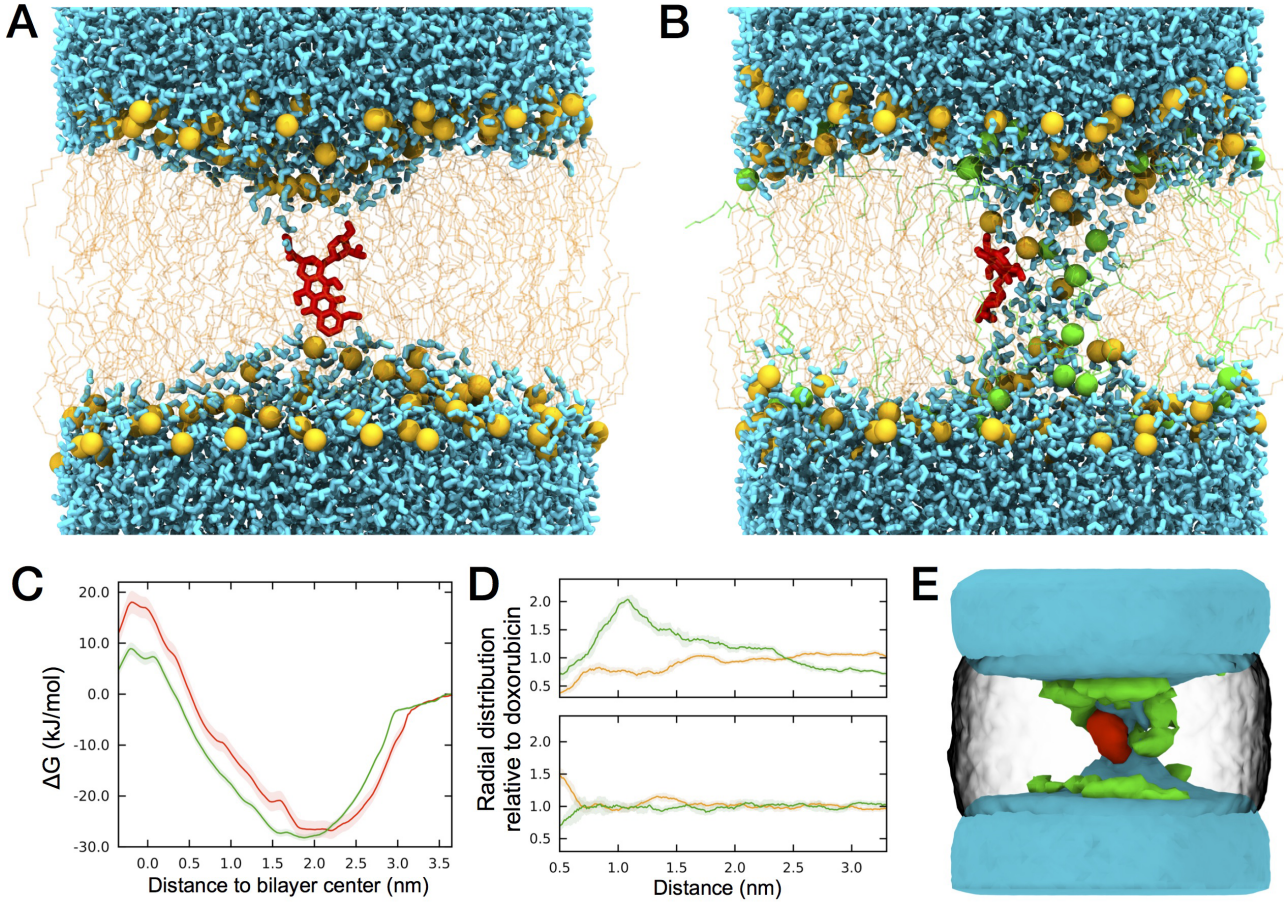

Figure 2 | Short-chain phosphatidylcholines dynamically assemble into a molecular gateway for doxorubicin. (A), (B) Snapshots of simulations of a pure DPPC bilayer (A) or a 4 : 1 DPPC:DOctPC bilayer (B). Doxorubicin was localized at the center of the bilayer by a harmonic potential. During doxorubicin traversal, the short-chain lipids assemble a transient membrane channel. Doxorubicin is in red, water in blue, DPPC in yellow and DOctPC in green; lipid headgroups are represented by a single bead at the phosphorus position. (C) The energetic barrier for doxorubicin translocation is reduced by the short-chain lipids. Potential of mean force for doxorubicin as a function of the distance to the center of the membrane. Pure DPPC (red) or DPPC:DOctPC (4 : 1) (green) bilayers; ±SD (shaded bands). (D), (E) Radial distribution for DOctPC (green line), relative to the doxorubicin position (D) DPPC (orange line) is plotted as a control. In the top plot, doxorubicin located in the bilayer center, showing an enrichment of the DOctPC in the vicinity of doxorubicin. The bottom plot represents the situation where doxorubicin localizes at the position of minimal membrane disturbance (water-lipid bilayer interface), which showed absence of co-localization for DOctPC with doxorubicin. (E) Corresponding volumes of occupancy (>10%) over a 120 ns time period. Doxorubicin in red, DOctPC in green, DPPC in translucid gray and water in blue.

preferred association with the short-chain lipids was observed (Fig. 2D, lower panel). In contrast, when doxorubicin positioned in the bilayer hydrophobic core, the short-chain lipids self-assemble in its vicinity, adapting to doxorubicin (Fig. 2D, upper panel). The notion that doxorubicin triggered channel formation was supported experimentally, as short-chain lipids without doxorubicin did not affect membrane permeability and GC instead significantly stabilized the membrane in an erythrocyte lysis assay (Fig. S2).

To further elucidate the self-assembling behavior of the short-chain lipids, the space occupancy of the different molecules was averaged over a time period of 120 ns, as shown in Fig. 2E (see also Movie S2). Short-chain lipids preferentially twisted around the doxorubicin molecule and localized at the curvature of the channel. The data show that self-assembly of short-chain lipids, triggered by doxorubicin's infringement of normal lipid order, forms a transient channel for the doxorubicin to traverse the membrane.

GC improves doxorubicin therapy and overcomes multi-drug resistance in a heterogeneous GEM mammary tumour population. As the above-described mechanism of membrane channel formation is unrelated to drug resistance mechanisms involving transporter proteins, we predicted that the lipid channels would thus be able to counteract unresolved conditions of multi-drug resistance. The WAPcre;Ecad$^{F/F}$;p53$^{F/F}$ (WEP) mammary tumour model is a genetically engineered mouse (GEM) model that closely mimics human invasive lobular breast carcinoma (ILC)[15,16]. To characterize the drug sensitivity of the Ecad$^{-/-}$;p53$^{-/-}$ WEP tumours, we set up a mouse clinical trial by transplanting series of individual WEP tumours into syngeneic recipient female mice. Thus, a heterogeneous population of mammary tumour-bearing mice was established, albeit within the limits of a defined, clinically relevant breast cancer subtype (ILC). Mice with tumours of 200 mm^3 were selected for treatment at maximum tolerated dose and randomized against untreated controls. Conventional chemotherapeutics (doxorubicin, docetaxel, topotecan, cisplatin) were administered as well as the poly(ADP-Ribose) Polymerase (PARP) inhibitor olaparib.

The large variations (SEM), already evident from the control group, reflect the inter-individual heterogeneity characteristic for the set-up (Fig. 3). Although some of the mice responded to cisplatin therapy, overall these tumours appeared resistant towards chemotherapy, and to (free) doxorubicin in particular (Fig. 3).

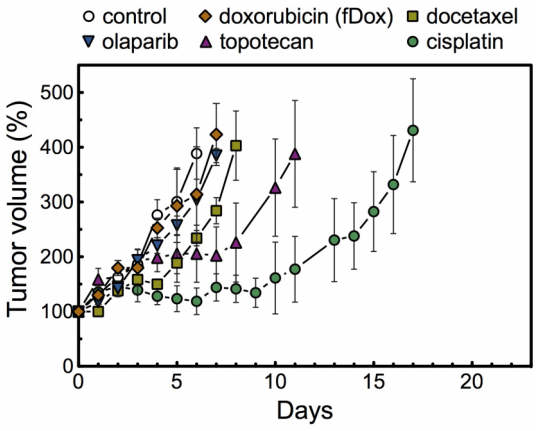

Figure 3 | Ecad$^{-/-}$;p53$^{-/-}$ GEM mammary tumours are multi-drug resistant. After orthotopic transplantation of a population of spontaneous tumours from WAPcre;EcadF/F;p53F/F mice, treatment was started with the indicated cytostatic drugs when tumour size reached 200 mm^3, all at maximum tolerated dose (MTD); or mice were left untreated as controls. (Mean, SEM, n = 5).

We next investigated whether the induction of transient membrane channels by GC would sensitize to doxorubicin therapy. As GC in its free form is not water soluble, GC was co-formulated with liposomal doxorubicin (LDox GC), without affecting the main pharmaceutical parameters of the carrier[17]. Due to the outer PEG shielding, the liposomes do not directly interact or fuse with cells[8]. However, GC transfers from the liposomes via the aqueous phase into the cell membrane (ref. 18, Fig. S3), thus remaining available to the tumour cell membrane. Cell lines were derived from untreated WEP Ecad$^{-/-}$;p53$^{-/-}$ mammary tumours. Pre-incubation of these WEP cell cultures with free GC elevated intracellular doxorubicin accumulation in a GC dose-dependent fashion (Fig. 4A). We subsequently tested liposomal doxorubicin with and without 10 mol% GC incorporated into its liposome bilayer on the WEP cells. LDox was of the same composition as commercial Caelyx® (Doxil®) used in the clinic. In line with its clinical features, LDox poorly delivered its contents into the WEP cells, even after 24 hours incubation. In contrast, LDox GC established substantial intracellular doxorubicin levels, an 8-fold increase over conventional LDox (Fig. 4B, C), and the increased intracellular doxorubicin accumulation correlated with improved cytotoxicity (Fig. 4D). As a control, empty liposomes of the same lipid composition but without doxorubicin showed no cytotoxicity at all in the same concentration range for either formulation (data not shown). Also in other WEP cell lines a similar gain of cytotoxicity by LDox GC was observed, up to EC50 values obtained by free doxorubicin (Table S2).

After establishing efficacy in the WEP cultures in vitro, we assessed therapy response in the GEM model, using the clinical trial set-up, as described above. The clinically used doxorubicin formulations free doxorubicin (fDox) and conventional liposomal doxorubicin (LDox) were administered at MTD, LDox GC was applied at equidose to LDox (10 mg/kg), while untreated tumours served as control. As depicted in Fig. 5A, LDox (without GC) generated an initial anti-tumour effect, more so than free doxorubicin (fDox), but tumours finally progressed despite additional dosing in either group. However, when GC is present (LDox GC; 10 mg/kg) a sustained inhibition of tumour progression was observed. At day 21 of treatment in the LDox GC group, tumour size was significantly reduced over LDox ($p < 0.05$), by two-fold (Fig. 5A).

We subsequently analyzed the overall survival of the different treatment cohorts. The clinically used doxorubicin formulations (LDox and fDox) did not result in a significantly extended survival over the control group. Importantly, LDox GC was the only intervention that prolonged overall survival significantly over untreated controls ($p = 0.001$). Median survival extended from 11 days to 30 days (Fig. 5B). A separate study in a homogeneous tumour cohort, established from a single WEP donor tumour (CDB212) randomly selected from the population a priori, further underlined these results (Fig. S4).

After study exit, all major organs were collected and the samples were blinded for investigation by veterinary pathologists. The LDox GC group revealed minimal normal tissue effects; no additional toxicities were discernable as compared to the other doxorubicin formulations. In all groups, the most prevalent anomaly was depleted erythropoiesis, (Fig. 5C, right panels) in bone marrow (upper panels) and spleen (lower panels), as compared to a healthy tumour-free (FVB × 129/Ola) F1 mouse (left panels). In addition to tumour-induced anemia, enforcement of this pathology by doxorubicin is a well-known adverse effect, also in the human situation[19,20]. Notably, for LDox GC this normal tissue effect was less frequent, as compared to the LDox treated group (Fig. 5D). In the LDox GC cohort, the incidence of reduced erythropoiesis appeared not significantly elevated, compared to untreated controls (Chi-square test: $p = 0.41$), in contrast to the LDox treatment (Chi-square test: $p = 0.036$). Overall, we conclude that GC counteracts chemotherapy resistance in a

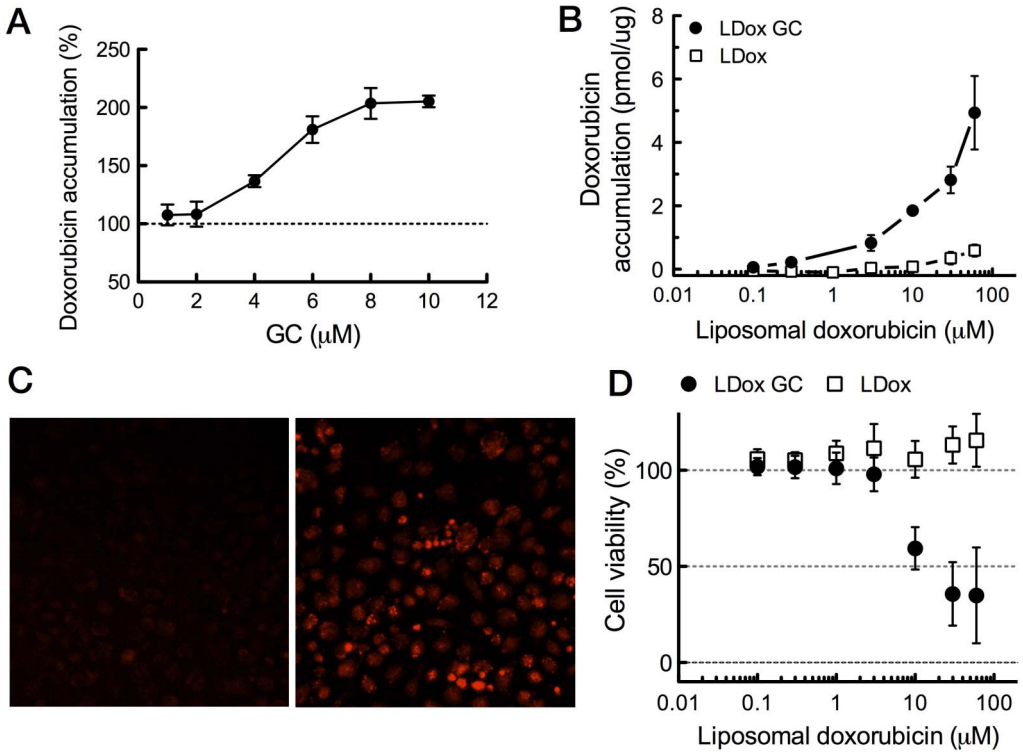

Figure 4 | GC enhances cellular accumulation of doxorubicin in mouse mammary tumour (WEP) cells and restores cytotoxicity. (A–C) Intracellular doxorubicin accumulation in WEP cells in presence or absence of GC. WEP3 cell cultures were derived from Ecad$^{-/-}$;p53$^{-/-}$ mammary tumours and were pre-incubated with free GC from an ethanol solution, followed by 1 hour free doxorubicin incubation (50 μM) (A) Intracellular doxorubicin accumulation was quantified by fluorometry on cell lysates and normalized against control (no GC pre-incubation). (B) Doxorubicin accumulation in WEP3 cells incubated for 24 hours with liposomal doxorubicin plus GC (LDox GC), or conventional doxorubicin liposomes (LDox) as control. (C) Fluorescence micrographs of doxorubicin, taken at equal exposure times, on (live) WEP3 cells immediate after 24 hours incubation with LDox GC (right panel) or LDox (left panel) (10 μM). (D) WEP3 cell viability after 24 hour incubation with LDox GC or LDox. Cells were kept in culture for an additional 48 hours. Viability was then assessed by the metabolic XTT assay. Data are expressed as mean percentages to untreated cells (SD, n = 6). As a control, incubation with the same liposomes but devoid of doxorubicin did not affect cell viability.

clinically relevant tumour model, greatly improving efficacy at reduced bone marrow and spleen toxicity.

GC elevates intracellular doxorubicin accumulation in the GEM mammary tumour, while reducing normal tissue exposure. In order to further elucidate the observed reduced toxicity and to shed more light on the pharmacokinetics of LDox GC, doxorubicin plasma profiles were determined (CDB212 cohort). Evidently, the sustained circulation time of LDox was preserved upon GC co-formulation (Fig. 6A), while doxorubicin plasma levels steeply declined during the first two hours. Non-compartmental kinetic analysis showed that the distribution rate in this first phase increased 4-fold as compared to LDox without GC (Table S3), which mainly accounted for the reduced systemic doxorubicin levels. Overall, plasma AUC was reduced 3-fold ($p < 0.05$) and residual circulating doxorubicin (96 hours after administration) was decreased 8-fold ($p < 0.05$) by GC co-administration.

Once inside the cell, doxorubicin strongly binds DNA in the nucleus (75% of the total intracellular fraction)[21]. We investigated the intracellular accumulation of doxorubicin in the mammary tumour using the CDB212 cohort. In order to distinguish intracellular doxorubicin from the total tissue, we optimized a nucleus isolation protocol, minimizing doxorubicin carryover from the liposomes to less than 0.5%. The biodistribution was analyzed for each doxorubicin formulation over a time period that covered >90% plasma AUC (96 hours for both liposomal, 4 hours for the free doxorubicin).

fDox accounted for marginal total tumour as well as intracellular doxorubicin accumulation (Fig. 6B). Total tumour levels by LDox were high, but doxorubicin poorly entered the tumour cell (<15% of total tumour AUC), in line with its clinical limitations[22]. The accumulation of liposomes in the tumour tissue is attributed to 'Enhanced Permeability and Retention'[23], an effect observed for both liposomal formulations (Fig. S5). LDox GC however, at lower total tumour tissue level than LDox, strongly elevated intracellular doxorubicin (40% of total AUC), increasing the total intracellular accumulation by two-fold ($p < 0.05$) (Fig. 6B). Contrary to the tumour – the heart, liver and spleen showed comparable or even slightly (10–20%) reduced doxorubicin accumulation by GC co-administration (Fig. 6B, Table S4). Total tissue accumulation in the latter organs, active in clearing liposomal particles from the blood stream (reticuloendothelial system), was strongly reduced for LDox GC (Fig. 6B) – in concordance with its lower plasma levels (Fig. 6A). The decreased doxorubicin accumulation in the spleen is moreover in good agreement with the lower incidence of erythropoietic depletion by LDox GC (Fig. 5C, D).

We investigated whether there was a preference of GC mediated drug gateways for the tumour cell membrane. Of spleen, heart and tumour we determined the fraction doxorubicin that finally passes the membrane, ending up inside the cell, over the above mentioned time courses. The effect of GC appeared strongest on the tumour cell membrane (Fig. S6A). We confirmed this observation in vitro on various cell cultures (Fig. S6B).

Discussion

Membrane translocation strongly delineates the compounds that, from the vast chemical space, can potentially act as a bioactive drug.

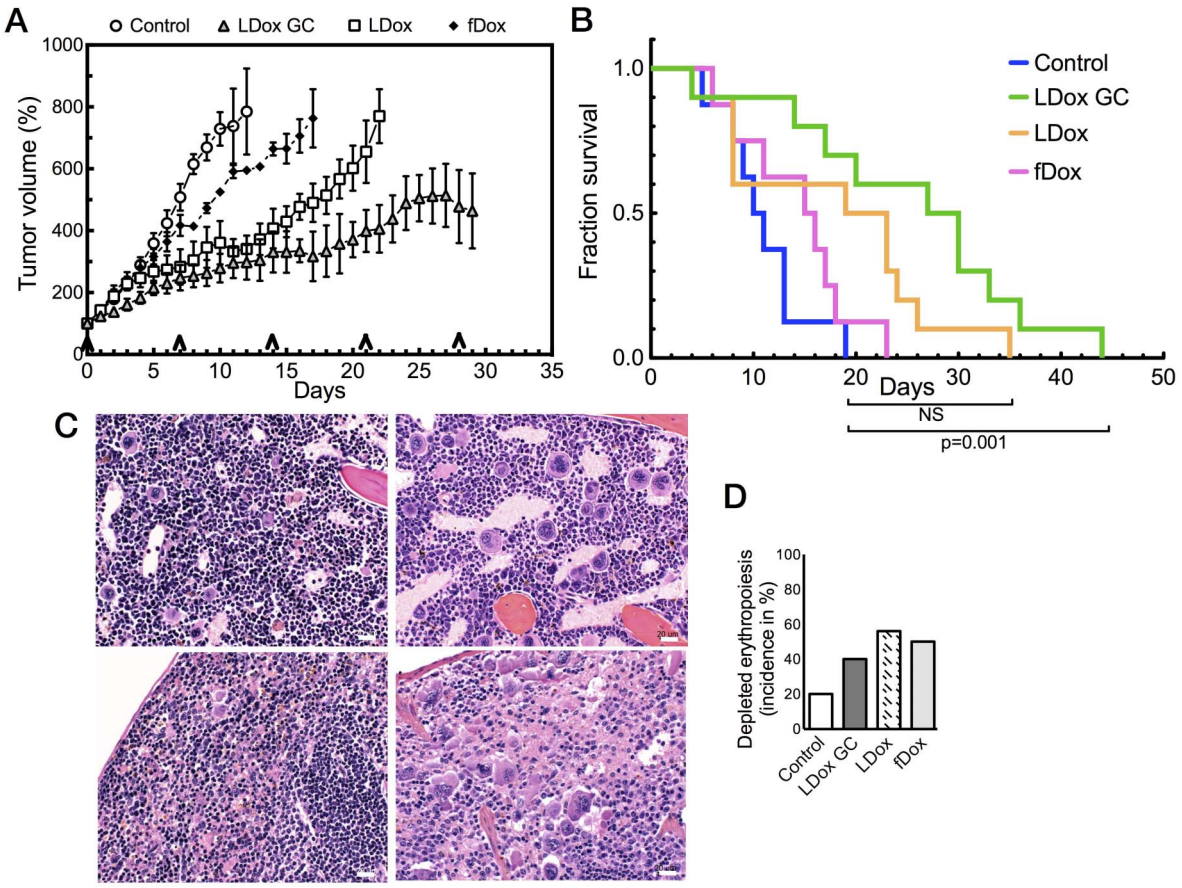

Figure 5 | Co-administration of GC provides superior anti-tumour efficacy in multi-drug resistant mammary tumours. (A) GC re-sensitize tumours to doxorubicin therapy in a heterogeneous tumour population; in the LDox GC cohort, average tumour size (±SEM, n = 9) was significantly reduced at day 21, compared to LDox (without GC) ($p < 0.05$). Arrows indicate time points of drug dosing. (B) LDox GC is the only treatment that significantly prolongs median survival by 2.7-fold over untreated control ($p < 0.001$). (C) H&E stained specimen of bone marrow (C, upper) and spleen (C, lower). Doxorubicin treatment severely depletes erythropoietic cells (dark-blue stained) (C, right), compared to control tissue (C, left) (bars 20 μm). (D) Incidence (%) of reduced erythropoiesis in numbers of organs per treatment group. Compared to control (6/30), depletion of erythropoiesis was seen in fDox (12/24) and LDox (18/32) groups, but less for GC co-administration (12/30).

Moreover, it hampers efficacy of existing drugs. Poor intracellular accumulation accounts for situations of suboptimal or ineffective therapy, including therapy resistance[24]. We here describe a well-defined paradigm for enhancing drug-membrane translocation and subsequent elevated intracellular accumulation. Amphiphilic drug molecules by themselves impose strong distortion upon the natural lipid assembly, when traversing the membrane. We demonstrate that during this process, the assembly of short-chain lipids is triggered around doxorubicin in a short time frame, much quicker (ns) than that of doxorubicin-membrane translocation (μs)[25]. Such spatiotemporal enrichment of the truncated lipids in vicinity of the drug favors local membrane curvature and hence allows transient channel formation of a size just fitting for doxorubicin to translocate. GC thus on its own does not permeabilize the membrane, and instead acts in rapid concert with the drug. After acceleration of the translocation process, channel disassembly can occur as soon the drug has left the membrane to bind its intracellular target or further diffuse through the body.

Liquid-disordered and liquid-ordered phases coexist in plasma membranes dependent on cell type and conditions[26]. The anti-cancer drug doxorubicin binds strongest to the liquid-ordered lipid phase of membranes[27]. Strikingly, the doxorubicin uptake-enhancing effect of GC is most prominent in the liquid-ordered (lipid raft) environment, where spontaneous doxorubicin traversal is slowest. In all tumour cells tested thus far, but not in most normal cells, lipid analogues (such as GC) effectively facilitated doxorubicin traversal across the plasma membrane. Characteristically, the outer leaflet of the plasma membrane is indeed enriched in sphingolipids and sterols[1], which form the liquid-ordered phase. One could therefore hypothesize that tumour cells are particularly rich in liquid-ordered plasma membrane outer leaflets, when compared to cells of e.g. heart, spleen and liver, as lipid compositions vary significantly between tissues and cell types[28–30]. However, systematic lipidomics information is lacking, and in particular at such subcellular detail. Advanced lipidomics analyses (e.g. by imaging mass spectrometry) are needed to further elucidate (subtle) differences among cell types, or those associated with malignant transformation[30–32].

Overall, rational design of lipid analogues, medicinal chemical lipid-analogue structure optimization, and systematic high-throughput screening are approaches that are suitable for identifying selected action on cell type and the drug combination of interest. For tumour cells, we are currently employing this strategy to improve efficacy of other anti-cancer drugs, such as mitoxantrone, which is clinically hampered by inadequate delivery and bioavailability.

Conventional therapy with free or liposomal doxorubicin has its limitations: Free doxorubicin shows life-threatening cardiotoxicity and is rapidly eliminated from the body[22]. Conventional liposomal doxorubicin (Caelyx®) stays sufficiently longer in circulation but is hampered by poor intracellular delivery of the drug[9,22]. A strategy of concomitant GC membrane targeting combines the advantages of

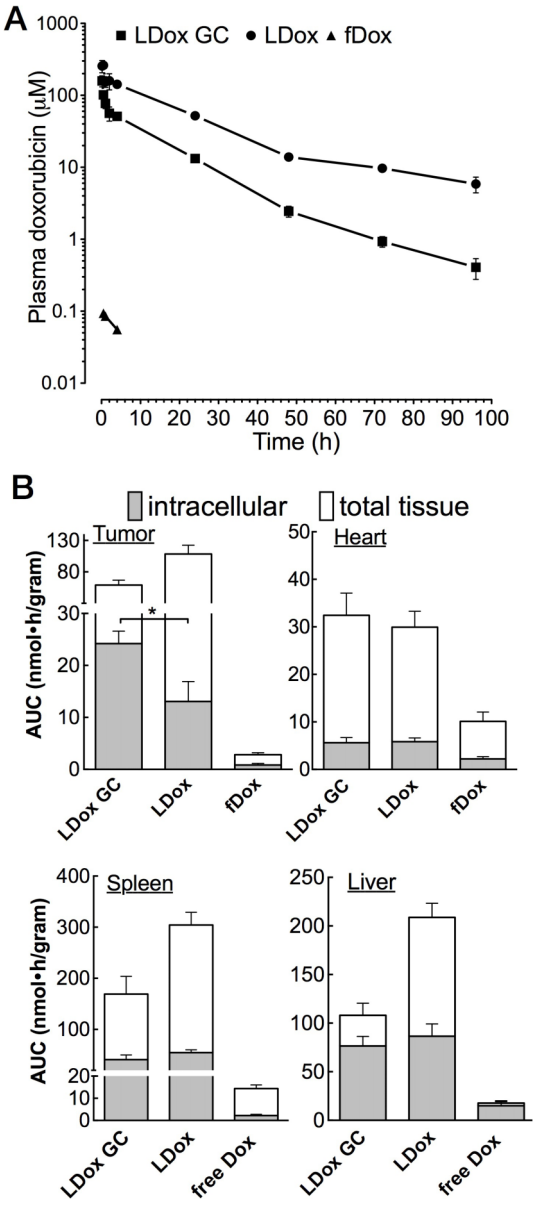

Figure 6 | GC reduces systemic exposure to doxorubicin, while elevating intracellular tumour accumulation. (A) Semi-logarithmic doxorubicin plasma concentration-time curve after i.v. injection of LDox GC, LDox and fDox. Plasma levels (μM) were expressed per injected dose (mean, SEM, n = 3). (B) Intracellular and total tissue doxorubicin in the tumour and the heart. Data are expressed as the AUC per gram tissue, per gram injected doxorubicin. GC elevates intracellular drug accumulation in the tumour by a factor two ($p < 0.05$). (Mean, SEM, n = 12).

these two clinical formulations (Fig. 7). While long-circulation is preserved by liposomal entrapment, GC establishes intracellular delivery into the tumour cells. Moreover, towards normal tissues doxorubicin exposure is unaffected or reduced, and plasma levels as well as erythropoeitic toxicity attenuate; resulting in an increase of the therapeutic ratio.

Liposomal encapsulation protects from life-threatening cardiotoxicity. As was evident from phase III clinical trials, this beneficial effect is rather independent of pharmacokinetics of the particular liposomal formulation[9,33]. In contrast, palmar-plantar erythrodysesthesia (PPE), the dose-limiting toxicity of current liposomal doxorubicin (Caelyx) therapy, strongly correlates to pharmacokinetics, in particular to long-term doxorubicin plasma level[34], which was 8-fold reduced by the co-formulation of GC.

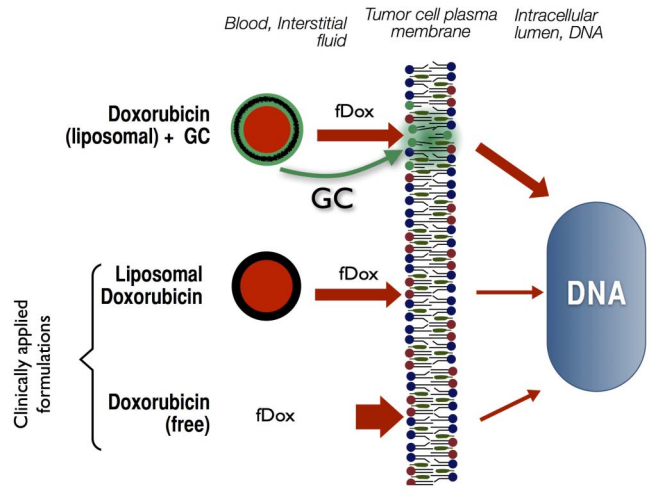

	LDox GC	LDox	fDox
long circulation	+	+	-
fraction intracellular doxorubicin (tumor)	++	-	+
normal tissue sparing	+	+/-	-

Figure 7 | Increased therapeutic window of doxorubicin by GC-mediated membrane modulation. From the liposomal vehicle, fDox (red) and free GC (green) leak into the interstitial fluids and partition into the (tumour) cell membrane (top cartoon). fDox plasma peak levels are much reduced by liposomal formulation (thinner red arrows left of membrane), but doxorubicin entry in the tumour cell is low in absence of GC (middle cartoon). GC, when co-inserted into the membrane, enhances membrane traversal of doxorubicin (thickened red arrow right of membrane) and thus, accumulation into tumour cell DNA. The relative effects of the three doxorubicin formulations on blood circulation time, tumour cell nucleus incorporation and sparing of normal tissues are summarized in the table.

We used Ecad$^{-/-}$;p53$^{-/-}$ mouse mammary tumours that, like many other spontaneous GEM tumours, are therapy resistant and closely resemble the human counterpart[15,16]. Uptake of free doxorubicin by these tumours was extremely low. LDox GC may challenge therapy resistance of these tumours in three ways. First, the liposomes accumulate in the tumour over time, a phenomenon known as Enhanced Permeability and Retention[23], thereby reaching substantially higher doxorubicin levels in tumour tissue than with free doxorubicin. Secondly, the short-chain lipid enhances the doxorubicin flux into the tumour cell from the interstitial fluid where the liposomes leak their content. Thirdly, the efficacy of GC may be enforced by the fact that multidrug-resistance (MDR) proteins (such as the ABCB1 and ABCC1 drug efflux transporters) are lipid exporters that expel short-chain GC (but not long-chain GC) efficiently to the outer bilayer leaflet[35], once it has reached the intracellular side after co-flipping with doxorubicin. The short-chain lipid is thus continuously recycled back to the cell surface, ready to aid new doxorubicin partners in traversing the membrane. This study highlights a critical role of the cellular plasma membrane in cases of drug resistance.

In summary, drug-triggered molecular assembly of transient channels facilitates drug traversal over the plasma membrane. GC-mediated channels preferentially target the tumour cell membrane to strongly elevate intracellular doxorubicin accumulation. While reducing systemic exposure, LDox GC increases anti-tumour efficacy and overcomes multi-drug resistance.

Methods

Doxorubicin uptake. Serum-starved BAEC cells were pre-incubated with short-chain lipids from ethanol for 15 minutes after which free doxorubicin was applied for 1 hour. Intracellular doxorubicin was quantified and corrected for protein content.

Assay for doxorubicin translocation across lipid vesicles. By reversed-phase evaporation large unilaminar vesicles (LUV) were prepared to enclose DNA. The DNA-LUVs were injected into a doxorubicin solution (50 μM) and doxorubicin fluorescence was monitored in a spectrofluorometer. The quenching of fluorescence (Q) over time was fitted according to Q(t) = Q(max)t/(K(translocation) + t), where K(translocation) is the translocation half-time (sec). The maximal quenching (Q(max)) was determined after releasing all DNA by LUV disruption.

Molecular dynamics of doxorubicin translocation. Simulations of doxorubicin translocation across a membrane containing 1,2-dipalmitoyl-sn-glycero-3-phosphocholine (DPPC) or DPPC and 1,2-dioctanoyl-sn-glycero-3-phosphocholine (DOctPC) were carried out using GROMACS 4.5.4 package and 53A6 GROMOS united-atom force field. The center of mass of doxorubicin was positioned at different distances to the bilayer center, as indicated, using a harmonic restraint in the direction of the bilayer normal. Free energy profiles were obtained after integrating the force of the restraining potential at each depth.

GEM mammary tumour model and therapeutic intervention. Ecad$^{-/-}$;p53$^{-/-}$ mammary tumours, generated in WAPcre;EcadF/F;p53F/F (WEP) mice were orthotopically transplanted in syngeneic wild-type mice. The first drug dose was administered when the tumour reached 200 mm^3. The tumour volume (in mm^3) was calculated using the formula: 0.5 × length × width2. Treatments (MTD): Olaparib: daily 50 mg/kg i.p.; docetaxel: weekly 25 mg/kg i.v.; cisplatin: once every two weeks 6 mg/kg i.v.; topotecan daily 4 mg/kg i.p.; free doxorubicin: weekly 5 mg/kg i.v.; LDox (conv): weekly 10 mg/kg i.v.; LDox GC: weekly 10 mg/kg i.v. Mice were sacrificed when tumour volume exceeded 1500 mm^3 or body weight declined below 80% of its initial value. Tissues, including mammary fat pad (tumour), sentinel lymph node, lung, liver, heart, bone marrow, thymus, spleen, kidneys and GI-tract, were blinded, fixed and H&E stained followed by pathological investigation. All mouse experiments were performed in accordance with Dutch law and regulatory guidelines. The 'Dier Experimentele Commissie' of the NKI was involved in experimental design and approved all experiments prior to study start.

Plasma kinetics. From mice with the CDB212 tumour (350 mm^3) blood samples were drawn by tail-clipping and collected in heparinized tubes. Plasma was obtained and doxorubicin was quantified by HPLC and expressed per gram injected doxorubicin.

Doxorubicin incorporation in tissues and cell nuclei. Mice with orthotopical CDB212 tumours were i.v. injected with doxorubicin when primary tumour was 350 mm^3. At t = 4, 24, 48 and 96 hours (LDox GC and LDox) or at t = 0.5, 1 and 4 hours (fDox) 3 mice were sacrificed. Body perfusion was immediately performed (5 min, 100 mm Hg) via the left ventricle of the heart. Heart, liver, spleen and tumour tissue were homogenized in ice-cold nuclear isolation medium. From half of the sample nuclei were isolated by sucrose density centrifugation. Doxorubicin was quantified by HPLC. Data were corrected for tissue weight and doxorubicin dose, and if applicable, nuclei isolation yield.

1. van Meer, G., Voelker, D. R. & Feigenson, G. W. Membrane lipids: where they are and how they behave. *Nat. Rev. Mol. Cell. Biol.* **9**, 112–124 (2008).
2. Finkelstein, A. Water and nonelectrolyte permeability of lipid bilayer membranes. *J. Gen. Physiol.* **68**, 127–135 (1976).
3. Al-Awqati, Q. One hundred years of membrane permeability: does Overton still rule? *Nat. Cell. Biol.* **1**, E201–202 (1999).
4. Dobson, P. D. & Kell, D. B. Carrier-mediated cellular uptake of pharmaceutical drugs: an exception or the rule? *Nat. Rev. Drug. Discov.* **7**, 205–220 (2008).
5. Sugano, K. *et al.* Coexistence of passive and carrier-mediated processes in drug transport. *Nat. Rev. Drug. Discov.* **9**, 597–614 (2010).
6. Lankelma, J. *et al.* Doxorubicin Gradients in Human Breast Cancer. *Clin. Cancer Res.* **5**, 1703–1707 (1999).
7. Regev, R. & Eytan, G. D. Flip-flop of doxorubicin across erythrocyte and lipid membranes. *Biochem. Pharmacol.* **54**, 1151–1158 (1997).
8. Papahadjopoulos, D. *et al.* Sterically stabilized liposomes: improvements in pharmacokinetics and antitumor therapeutic efficacy. *Proc. Natl. Acad. Sci. USA* **88**, 11460–11464 (1991).
9. O'Brien, M. E. *et al.* Reduced cardiotoxicity and comparable efficacy in a phase III trial of pegylated liposomal doxorubicin HCl (CAELYX/Doxil) versus conventional doxorubicin for first-line treatment of metastatic breast cancer. *Ann. Oncol.* **15**, 440–449 (2004).
10. van Lummel, M. *et al.* Enriching lipid nanovesicles with short-chain glucosylceramide improves doxorubicin delivery and efficacy in solid tumors. *FASEB J.* **25**, 280–289 (2011).
11. Veldman, R. J., Zerp, S., van Blitterswijk, W. J. & Verheij, M. N-hexanoyl-sphingomyelin potentiates in vitro doxorubicin cytotoxicity by enhancing its cellular influx. *Br. J. Cancer* **90**, 917–925 (2004).
12. Israelachvili, J. N., Mitchell, D. J. & Ninham, B. W. Theory of self-assembly of hydrocarbon amphiphiles into micelles and bilayers. *J. Chem. Soc., Faraday Trans. 2* **72**, 1525–1568 (1976).
13. Orsi, M. & Essex, J. W. Permeability of drugs and hormones through a lipid bilayer: insights from dual-resolution molecular dynamics. *Soft Matter* **6**, 3797–3808 (2010).
14. de Wolf, F. A. *et al.* Comparable interaction of doxorubicin with various acidic phospholipids results in changes of lipid order and dynamics. *Biochim. Biophys. Acta* **1096**, 67–80 (1990).
15. Derksen, P. W. *et al.* Mammary-specific inactivation of E-cadherin and p53 impairs functional gland development and leads to pleomorphic invasive lobular carcinoma in mice. *Dis. Model. Mech.* **4**, 347–358 (2011).
16. Derksen, P. W. *et al.* Somatic inactivation of E-cadherin and p53 in mice leads to metastatic lobular mammary carcinoma through induction of anoikis resistance and angiogenesis. *Cancer Cell* **10**, 437–449 (2006).
17. Veldman, R. J. *et al.* Coformulated N-octanoyl-glucosylceramide improves cellular delivery and cytotoxicity of liposomal doxorubicin. *J. Pharmacol. Exp. Ther.* **315**, 704–710 (2005).
18. Futerman, A. H. & Pagano, R. E. Use of N-([1-14C]hexanoyl)-D-erythro-sphingolipids to assay sphingolipid metabolism. *Methods Enzymol.* **209**, 437–446 (1992).
19. Nurgalieva, Z., Liu, C. C. & Du, X. L. Chemotherapy use and risk of bone marrow suppression in a large population-based cohort of older women with breast and ovarian cancer. *Med. Oncol.* (2010).
20. Steinberg, D. Anemia and cancer. *CA: Cancer J. Clin.* **39**, 296–304 (1989).
21. Xiong, G., Chen, Y. & Arriaga, E. A. Measuring the Doxorubicin Content of Single Nuclei by Micellar Electrokinetic Capillary Chromatography with Laser-Induced Fluorescence Detection. *Anal. Chem.* **77**, 3488–3493 (2005).
22. Gabizon, A., Shmeeda, H. & Barenholz, Y. Pharmacokinetics of pegylated liposomal Doxorubicin: review of animal and human studies. *Clin. Pharm.* **42**, 419–436 (2003).
23. Fang, J., Nakamura, H. & Maeda, H. The EPR effect: Unique features of tumor blood vessels for drug delivery, factors involved, and limitations and augmentation of the effect. *Adv. Drug Del. Rev.* **63**, 136–151 (2011).
24. Borst, P., Jonkers, J. & Rottenberg, S. What Makes Tumors Multidrug Resistant? *Cell Cycle* **6**, 2782–2787 (2007).
25. Regev, R., Yeheskely-Hayon, D., Katzir, H. & Eytan, G. D. Transport of anthracyclines and mitoxantrone across membranes by a flip-flop mechanism. *Biochem. Pharmacol.* **70**, 161–169 (2005).
26. Lingwood, D. & Simons, K. Lipid rafts as a membrane-organizing principle. *Science* **327**, 46–50 (2010).
27. Adler, M. & Tritton, T. R. Fluorescence depolarization measurements on oriented membranes. *Biophys. J.* **53**, 989–1005 (1988).
28. Harkewicz, R. & Dennis, E. A. Applications of Mass Spectrometry to Lipids and Membranes. *Ann. Rev. Biochem.* **80**, 301–325 (2011).
29. van Meer, G. Atherosclerosis, endothelium and plasma membrane lipid polarity. *Agents Actions Suppl.* **26**, 15–25 (1988).
30. Sampaio, J. L. *et al.* Membrane lipidome of an epithelial cell line. *Proc. Natl. Acad. Sci. USA* **108**, 1903–1907 (2010).
31. Harkewicz, R. & Dennis, E. A. Applications of mass spectrometry to lipids and membranes. *Annu. Rev. Biochem.* **80**, 301–325 (2011).
32. Shevchenko, A. & Simons, K. Lipidomics: coming to grips with lipid diversity. *Nat Rev. Mol. Cell. Biol.* **11**, 593–598 (2010).
33. Harris, L. *et al.* Liposome-encapsulated doxorubicin compared with conventional doxorubicin in a randomized multicenter trial as first-line therapy of metastatic breast carcinoma. *Cancer* **94**, 25–36 (2002).
34. Lorusso, D. *et al.* Pegylated liposomal doxorubicin-related palmar-plantar erythrodysesthesia ('hand-foot' syndrome). *Ann. Oncol.* **18**, 1159–1164 (2007).
35. van Meer, G., Halter, D., Sprong, H., Somerharju, P. & Egmond, M. R. ABC lipid transporters: extruders, flippases, or flopless activators? *FEBS Lett.* **580**, 1171–1177 (2006).

Acknowledgements

We acknowledge Olaf van Tellingen and Levi Buil for their help with the doxorubicin HPLC analyses. We thank Piet Borst for critically reading the manuscript. This work was financially supported by the Dutch Cancer Society (KWF), grant NKI 2008-4113 and the European Research Executive Agency, grant FP7-PEOPLE-2009-IEF-254559.

Author contributions

A.v.H., M.M., W.v.B., M.V. wrote the paper; A.v.H., M.M., D.G., L.P., T.B. carried out research; J.S. analyzed data; A.v.H., G.A.K., W.v.B., S.M., J.J. and M.V. designed the research.

Additional information

Supplementary information accompanies this paper at http://www.nature.com/scientificreports

Competing financial interests: The authors declare no competing financial interests.

License: This work is licensed under a Creative Commons Attribution-NonCommercial-NoDerivs 3.0 Unported License. To view a copy of this license, visit http://creativecommons.org/licenses/by-nc-nd/3.0/

How to cite this article: van Hell, A.J. *et al.* Defined lipid analogues induce transient channels to facilitate drug-membrane traversal and circumvent cancer therapy resistance. *Sci. Rep.* **3**, 1949; DOI:10.1038/srep01949 (2013).